Hindawi Publishing Corporation
International Journal of Photoenergy
Volume 2013, Article ID 745301, 6 pages
http://dx.doi.org/10.1155/2013/745301

Research Article

A Novel Solar Driven Photocatalyst: Well-Aligned Anodic WO_3 Nanotubes

Chin Wei Lai,[1] Sharifah Bee Abd Hamid,[1] and Srimala Sreekantan[2]

[1] *Nanotechnology & Catalysis Research Centre (NANOCAT), Institute of Postgraduate Studies (IPS), University of Malaya, 3rd Floor, Block A, 50603 Kuala Lumpur, Malaysia*
[2] *School of Materials and Mineral Resources Engineering, Universiti Sains Malaysia, Engineering Campus, 14300 Nibong Tebal, Seberang Perai Selatan, Pulau Pinang, Malaysia*

Correspondence should be addressed to Chin Wei Lai; cwlai@um.edu.my

Received 6 July 2013; Accepted 25 August 2013

Academic Editor: Meenakshisundaram Swaminathan

Well-aligned anodic tungsten trioxide (WO_3) nanotubes were successfully synthesized by anodization of W foil at 40 V in a bath with electrolyte composed of 1 M of sodium sulphate (Na_2SO_4) and 0.5 wt% ammonium fluoride (NH_4F). The effect of electrochemical anodization times on the formation mechanism of anodic WO_3 nanotubular structure was investigated. It was found that minimum of 15 min is required for completing transformation from W foil to WO_3 nanotubular structure with an average diameter of 50 nm and length of 500 nm. The photocatalytic ability of the samples was evaluated by degradation of methyl blue (MB) dye. The results indicate that the surface morphology of anodic WO_3 affected the photocatalytic MB degradation significantly under solar illumination.

1. Introduction

Nowadays, global warming poses one of the most serious threats to the global environment ever faced in human history [1, 2]. Over the past ten years, titanium dioxide (TiO_2) photocatalyst has become one of the most studied materials for photocatalytic studies [3–8]. However, TiO_2 photocatalyst has wide band gap (3.0–3.2 eV), which exhibits poor responsive to visible light region [9–12]. Nevertheless, much literatures has reported that visible light driven TiO_2 photocatalyst could be achieved by doping sufficient content of cations or anions into the lattice of TiO_2 to create certain states within the band gap energy of TiO_2 [5, 9–15]. However, modification of TiO_2 photocatalyst has several drawbacks, such as thermal instability, and recombination centers for photoinduced charge carriers, which decrease the photocatalytic ability significantly [16–18]. These issues are still far from being solved. In line with this objective, many efforts and studies have been devoted to small band gap metal oxide semiconductor for strong absorption within solar spectrum [19–22].

Recently, WO_3 has gained much scientific interest because WO_3 is one of very few metal oxide semiconductor response to visible light illumination [19–25]. In addition, it exhibits a broad range of functional properties, such as its small band gap energy (2.4 eV to 2.8 eV), deeper valence band (+3.1 eV), stable physicochemical properties, and strong photocorrosion stability in aqueous solution [19–28]. In this manner, design and development of nanostructure of WO_3 assemblies have gained significant interest in recent years, especially one-dimensional nanotubular structure. However, several studies have reported that growth of well-aligned and uniformity of anodic WO_3 nanotubular structure was a difficult task and most of the studies only able to grow anodic WO_3 into nanoporous instead of nanotubular structure [19–25, 27]. To the best of our knowledge, the literature about the formation of well-aligned anodic WO_3 nanotubes in shorter time is still lacking. Therefore, considerable efforts have been devoted to grow the high uniformity and well-aligned anodic WO_3 nanotubes via electrochemical anodization technique. Such a mechanistic understanding is very important for the controlled growth of ordered WO_3 nanotubular structures, which may be used in several environmental applications to realize a green economy in our future.

2. Experimental Procedure

2.1. Preparation of Anodic WO_3 Nanostructures. Anodic WO_3 nanostructures were synthesized via electrochemical anodization of W foil (99.95% purity, 0.1 mm in thickness, Alfa Aesar, USA) in a bath with electrolytes composed of 100 mL of 1 M of sodium sulfate (Na_2SO_4, Merck, USA) solution with 0.5 wt% of ammonium fluoride (NH_4F, Merck, USA) at 40 V with sweep rate of 1 V/s. Anodization process was performed in a two-electrode cell with W foil as the anode and the platinum rod as the counter electrode. The effect of anodization times on the formation of anodic WO_3 nanostructures was investigated (e.g., 2 min; 5 min; 10 min; 15 min; 30 min; and 60 min). After anodization process, anodized W foils were cleaned using acetone (J. T. Baker, Nederland) and dried in nitrogen stream.

2.2. Characterization of Anodic WO_3 Nanostructures. The morphologies of anodic WO_3 nanostructures were observed by field emission scanning electron microscopy (FESEM), using a FEI Quanta 200 (FESEM model, USA) at a working distance of around 1 mm. The cross-sectional observation was carried out on mechanically bent samples to get the thickness of the oxide layer. The chemical stoichiometry of the sample was characterized using energy dispersive X-ray (EDX) analysis, which is equipped in the FESEM. The morphologies of anodic WO_3 nanotubular structure were further confirmed by transmission electron microscope (TEM), using FEI CM 12 transmission microscope.

2.3. Photocatalytic MB Dye Degradation Studies. The photocatalytic MB dye degradation studies were conducted by dipping 4 cm^2 of anodic WO_3 nanostructures samples into a 100 mL of custom-made photoreactor consisting of quartz glas tube containing 30 ppm of MO dye solution. A blank sample (without anodic WO_3) was also prepared in order to eliminate the effect of the light towards the degradation of MB dye solution. Both samples were left in the reactor for 30 min in dark environment to achieve the adsorption/desorption equilibrium. It was then photoirradiated at room temperature by using a 150 W Xenon solar simulator (Zolix LSP-X150, China) with intensity of 800 W/m^2. 5 mL of MB dye solution was withdrawn for every 1 h from both quartz tubes to monitor the degradation of MB dye after irradiation. The concentration of the degraded MB dye solution was determined using UV-Vis spectrometer (PerkinElmer Lambda 35, USA).

3. Results and Discussion

In this part of the experimental study, the effect of anodization time on the morphology of anodic WO_3 oxide is discussed. Figure 1 shows FESEM images of the surface morphologies of anodized W foils in different anodization times. As shown in these FESEM images, the appearance of anodic oxides was dependent on the anodization times. Prior to the anodization process, the W foil was degreased by sonication in acetone and analyzed via FESEM. It could be observed that the W surface was relatively smooth and without any pits or pores on its surface (Figure 1(a)). As determined through EDX analysis, the pure W foils consisted of 100 at% of W (Table 1), which indicate that only W element was present without any impurities. The FESEM images of anodized W foils for different anodization times are shown in Figures 1(b) to 1(j). The inset of FESEM images showed the higher magnification of oxide layer on the surface of W foil. Interestingly, it was found that randomly small oxide pits were started to form on the W surface for 2 min of anodization (Figure 1(b)). Upon increasing the time to 5 min, these randomly small oxide pits were grown into larger pits (Figure 1(c)). For the sample anodized in 10 min, similar morphology of anodic WO_3 nanostructure was observed as compared to the sample anodized for 5 min (Figure 1(d)). However, these randomly oxide pits started to turn into larger pores structure and connect to each other to form a layer. This compact oxide nanoporous layer became more interconnected and eventually formed a uniform nanotubular structure as presented in Figure 1(e). The uniform nanotubular structure with an average diameter of ~50 nm and length of ~500 nm was successfully synthesized at minimum of 15 min (Figure 1(f)). Further increase in anodization time to 30 min and 60 min, the anodic WO_3 nanotubular structure was disappeared and only irregular nanoporous structure with thickness of ~100 nm could be observed (Figures 1(g)–1(j)). Representative samples (15 min anodized) were selected for the EDX and TEM analyses. The EDX analysis was employed to examine the chemical stoichiometry of the anodic WO_3 nanostructure. It was found that the atomic percentage of W element was about 54 at% whereas O element was about 46 at% (Table 1). Furthermore, the TEM image showed that hollow tube opening was obtained after electrochemical anodization process (Figure 2). It was found that the existence of the nanotubular structure with diameter of approximately 50 nm is further confirmed using TEM. Besides, the nanotubular wall thickness of approximately 10 nm could be observed.

Table 1: Average elemental compositions (at%) of pure W foil and anodic WO_3 nanostructures obtained in 1 M Na_2SO_4 electrolyte containing 0.5 wt% NH_4F for 15 min at 40 V obtained from EDX analysis.

Sample	W (at%)	O (at%)
Pure W foil (prior anodization)	100	—
Anodic WO_3 foil (15 min anodized)	54	46

In order to obtain the electrochemical information, a curve of current density versus time transient was plotted and presented in Figure 3. Such transient plot is important to explain the formation mechanism of anodic WO_3 nanostructures. In addition, the schematic illustrations on the possible stages undergone by the anodic oxide for the formation of the WO_3 nanotubular structure are shown in Figure 4. In this early stage of anodization, small oxide pits were started to form on the W surface randomly. These small oxide pits were formed through the hydrolysis process of W foil. The field-assisted migration of O^{2-} ions within the electrolyte through the W surface towards the W/WO_3 interface induce further growth of the oxide pits under applied voltage and longer

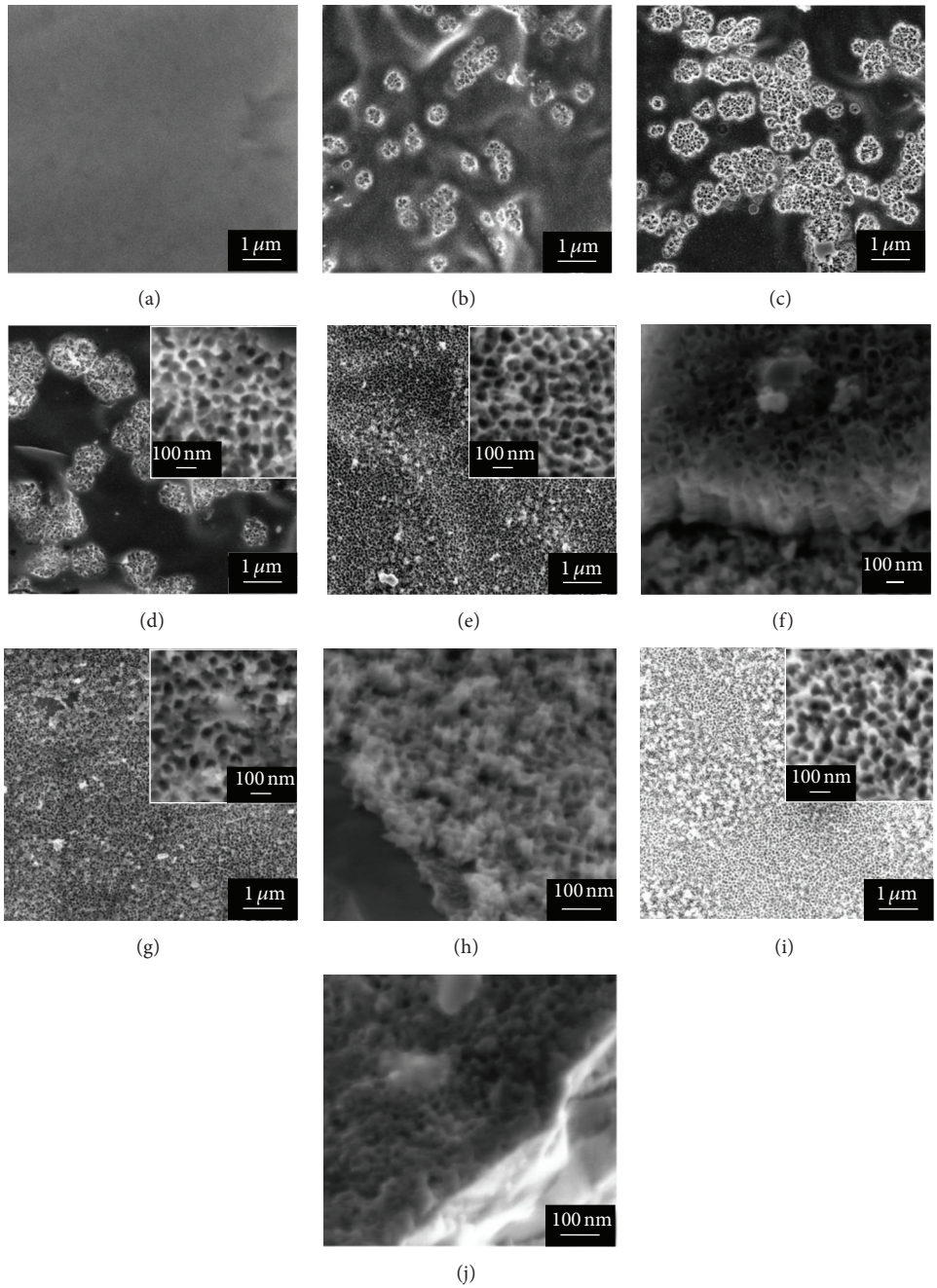

Figure 1: FESEM images of anodic WO_3 nanostructures obtained in 1 M Na_2SO_4 electrolyte containing 0.5 wt% NH_4F for different anodization times at 40 V: (a) pure W foil before anodization; (b) 2 min; (c) 5 min; (d) 10 min; (e) 15 min; (f) cross-sectional view for 15 min anodization; (g) 30 min; (h) cross-sectional view for 30 min anodization; (i) 60 min; (j) cross-sectional view for 60 min anodization. Insets show the higher magnification of the surface morphology.

anodization times [19, 23]. In this case, the resultant oxide pits will grow continuously until forming a compact oxide layer on W foil. The chemical reaction occurred is depicted as [$W^{6+} + 3H_2O \rightarrow WO_3 + 6H^+$]. Based on the current density curve, a dramatic decrease in current density mainly attributed to the poor electrical conductivity caused by the randomly oxide pits (stage A) [23, 25]. Meanwhile, the high electric field across the small oxide pits will subsequently induce the polarization of W–O bonding, which is strong enough to migrate W^{6+} ions and leave behind voids or pores [24, 27, 29]. These W^{6+} ions will dissolve into the electrolyte and eventually cause the porosification on the compact oxide layer. These pores or voids will be attacked by the tungsten fluorocomplex ions in the electrolyte, which induce chemical dissolution to enlarge and deepen pores and voids. It is a well-known fact that those fluorocomplex ions are the key factor in achieving regular nanostructure formation on valve metals via electrochemical anodization [8, 20–25, 27, 29–31]. The chemical

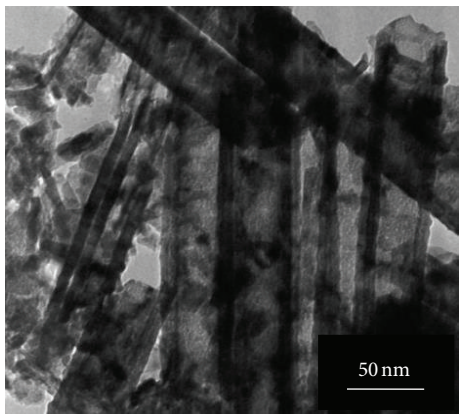

Figure 2: TEM image of anodic WO_3 nanostructures obtained in 1 M Na_2SO_4 electrolyte containing 0.5 wt% NH_4F for 15 min at 40 V.

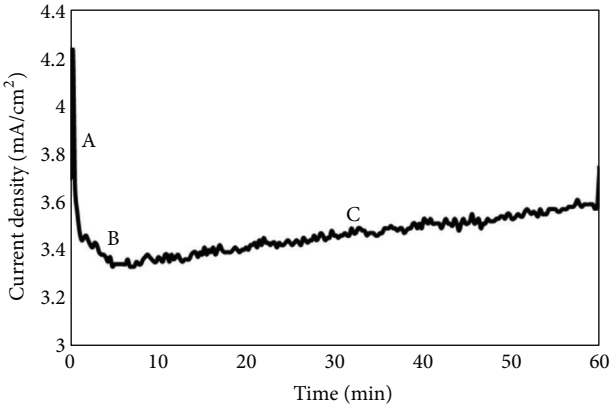

Figure 3: Current density versus duration response during the electrochemical anodization for 60 minutes at 40 V in 1 M Na_2SO_4 containing 0.5 wt% NH_4F.

Table 2: Selected samples for MB dye degradation based on different surface morphologies of anodic WO_3 samples via electrochemical anodization.

Sample	Anodization time	Morphological
A	10 min	Compact oxide layers with randomly pits
B	15 min	Nanotubular structure
C	30 min	Nanoporous structure

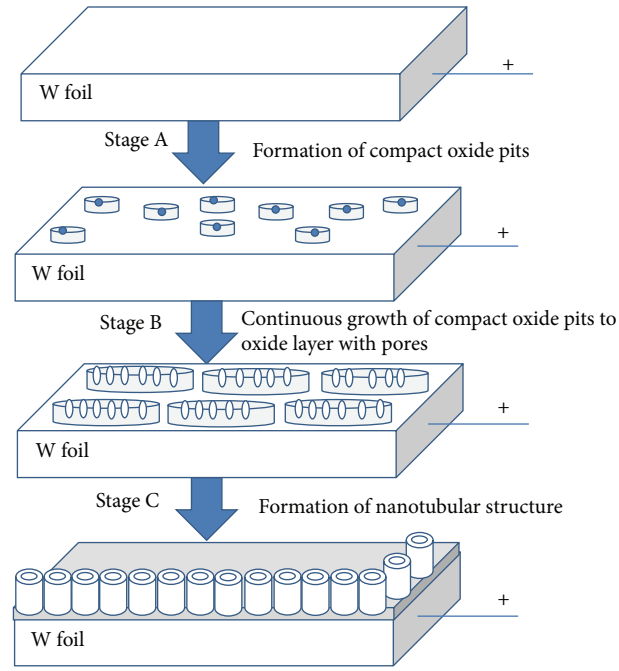

Figure 4: Schematic illustration of formation and mechanistic studies of anodic WO_3 nanostructures obtained in 1 M Na_2SO_4 electrolyte containing 0.5 wt% NH_4F for 15 min at 40 V.

reaction occurred in stage is depicted as [$WO_3 + 6H^+ + 8F^- \rightarrow (WF_8)^{2-} + 3H_2O$]. From the current density curve, the slight decrease in current density was due to the chemical dissolution by fluorocomplex ions as marked in Figure 3 (stage B). The small pores and voids on the compact oxide layers will grow inwards and eventually will form self-organized nanotubular structure. This is a result of equilibrium established between the electrochemical formation of WO_3 and its simultaneous chemical dissolution in fluoride containing electrolyte [22, 27]. Interestingly, the current density was increased slowly when the electrochemical anodization times prolonged (stage C). The reason might be attributed to the concentration of fluorocomplex ions in the electrolyte was decreased slowly for prolonging electrochemical anodization. In this manner, the balance between chemical dissolution and field-assisted dissolution and field-assisted oxidation will be interrupted and eventually will collapse the nanotubular structure and form nanoporous structure [19, 22]. In the present study, 15 min was found to be the optimum duration for the formation of self-organized circular nanotubular structure with lengths of approaching 500 nm.

The photocatalytic ability of selected anodic WO_3 samples formed via electrochemical anodization was evaluated by exposing MB organic dye under solar illumination as shown in Table 2. The changes in concentration of MB dye were analyzed as a function of exposure time (Figure 5). It was found that the concentration of the MB dye was decreased as the solar irradiation exposure time prolonged. The experimental results indicate that degradation of MB dye could be achieved in the present works. Based on the photocatalytic degradation results, the degradation rate in the presence of anodic WO_3 nanotubular structure (sample B) is much faster than the other samples. In addition, it could be noticed that the MB concentration was reduced from 30 ppm to ~7 ppm after 5 h solar irradiation assisted by sample B. It could be postulated that sample B has uniformity and apparent pore diameter throughout the photocatalyst surface; thus, more photocatalytic reactions could be triggered at the surface of the nanotubes (inner and outer wall surface) [7, 9, 12, 32]. Whereas, sample A has compact oxide layers with random pits on the surface of W foil. It showed lower photocatalytic degradation of MB organic dye among

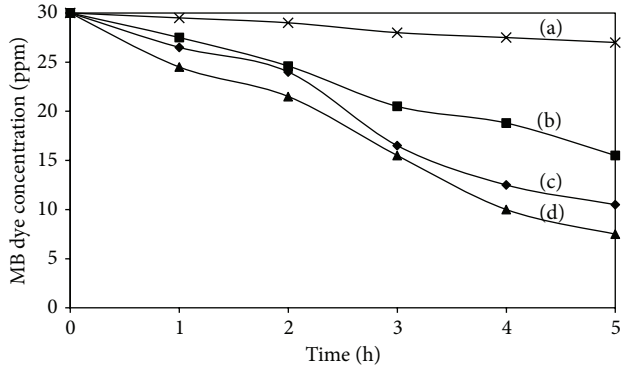

Figure 5: Photocatalytic degradation of MB dye solution under solar illumination, (a) blank sample (without anodic sample); (b) sample A (10 min); (c) sample C (30 min); and (d) sample B (15 min).

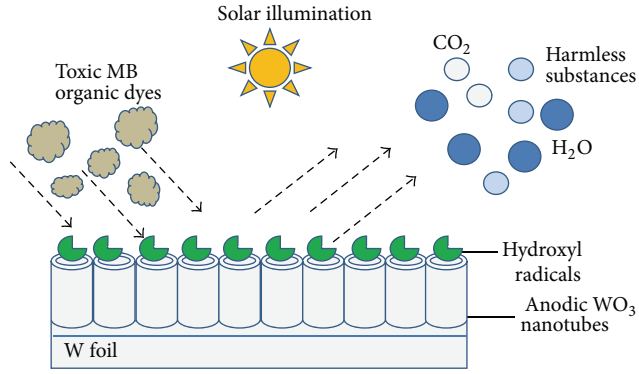

Figure 6: Schematic illustration of basic principal photocatalytic degradation of MB dye under solar illumination assisted by anodic WO_3 nanotubes.

the samples. This result manifested that the irregular thin compact oxide layers offer the small surface area for photons absorption from the solar irradiation. As a consequence, the generation of photoinduced charge carriers (electrons/holes pairs) from the anodic WO_3 was significantly decreased [7, 29, 30]. On the other hand, sample C has nonuniformity of nanoporous structure and exhibited slightly poor photocatalytic performance as compared to sample B. The reason mainly attributed to the numerous defects on the nanoporous structure, which could result in more recombination centers for electrons/holes pairs [5, 29]. Furthermore, the absorption of the photons from the solar illumination was limited in irregular nanoporous structure. Therefore, the number of photoinduced electrons/holes pairs was decreased and eventually leaded to poor photocatalytic degradation of MB dye.

In the present studies, MB molecule possesses a thiazine structure which contains polar atoms such as nitrogen, positively charge sulfur atom, and negatively charge chloride as counter ion [33, 34]. In this manner, anodic WO_3 photocatalyst possesses significantly higher surface acidity, thus, attracting more MB molecules for photocatalytic degradation reaction [21, 27]. In addition, the photocatalytic performance of a photocatalyst strongly depends on the ability to generate electrons/holes pairs, which will generate free radicals (hydroxyl radicals •OH) that are able to undergo secondary reactions [3, 4, 12]. A simple schematic illustration of basic principal in photocatalytic degradation of MB organic dyes is presented in Figure 6. In theoretical perspectives, anodic WO_3 photocatalyst generates two types of charge carriers (electrons/holes pairs) when absorption of high energy photons from solar illumination. The photons energy must be higher than band-gap energy of anodic WO_3 in order to generate electrons/holes pairs effectively [4, 9]. In ordinary substances, most of the electrons/holes pairs will recombine very fast by releasing energy in the form of unproductive heat or photons [18]. Based on the results obtained, anodic WO_3 nanotubular structure has a notable feature of strong oxidative decomposing power (positive holes) among the samples, which plays an important role in degrading the MB molecules. In the photocatalytic degradation studies, the oxidative decomposing power of positive charge holes is stronger than the reducing power of negative charge electrons. The strong oxidative process creates strong oxidation agent from the surface of photocatalyst in the presence of solar illumination and water [2–4, 22, 32]. This strong oxidation agent is released from the positive charge holes (valence band) after oxidizing the water molecules into hydroxyl radicals (•OH). Then, these •OH radicals will react with MB molecule and eventually decompose the toxic MB molecules into the harmless substances, carbon dioxide, and water [4, 32]. In conclusion, a novel anodic WO_3 nanotubular structure with high active surface area could generate more •OH radicals, which enhance the photocatalytic degradation of MB molecules under solar irradiation.

4. Conclusion

The present experimental work shows a strongly beneficial effect of anodic WO_3 nanotubular structure in enhancing the photocatalytic activity. It was found that a minimum of 15 min at 40 V via electrochemical anodization was required to form uniformity nanotubular structure in the electrolyte composed of 1 M of Na_2SO_4 and 0.5 wt% of NH_4F. The irregular anodic WO_3 nanoporous structure will be favored if the anodization time exceeded 15 min. A novel anodic WO_3 nanotubular structure is a cornerstone of green economy because it could degrade toxic MB organic dye effectively in the presence of solar illumination and water (renewable resources).

Acknowledgment

The authors would like to thank University of Malaya for funding this research work under University of Malaya Research Grant (UMRG), (RP022-2012D).

References

[1] J. A. Turner, "A realizable renewable energy future," *Science*, vol. 285, no. 5428, pp. 687–689, 1999.

[2] D. Mohan and C. U. Pittman Jr., "Arsenic removal from water/wastewater using adsorbents—a critical review," *Journal of Hazardous Materials*, vol. 142, no. 1-2, pp. 1–53, 2007.

[3] M. Kitano, M. Matsuoka, M. Ueshima, and M. Anpo, "Recent developments in titanium oxide-based photocatalysts," *Applied Catalysis A*, vol. 325, no. 1, pp. 1–14, 2007.

[4] A. Fujishima, X. Zhang, and D. A. Tryk, "TiO_2 photocatalysis and related surface phenomena," *Surface Science Reports*, vol. 63, no. 12, pp. 515–582, 2008.

[5] C. A. Grimes, "Synthesis and application of highly ordered arrays of TiO_2 nanotubes," *Journal of Materials Chemistry*, vol. 17, no. 15, pp. 1451–1457, 2007.

[6] S. Sreekantan and L. C. Wei, "Study on the formation and photocatalytic activity of titanate nanotubes synthesized via hydrothermal method," *Journal of Alloys and Compounds*, vol. 490, no. 1-2, pp. 436–442, 2010.

[7] Z. Su and W. Zhou, "Formation, morphology control and applications of anodic TiO_2 nanotube arrays," *Journal of Materials Chemistry*, vol. 21, no. 25, pp. 8955–8970, 2011.

[8] A. Ghicov and P. Schmuki, "Self-ordering electrochemistry: a review on growth and functionality of TiO_2 nanotubes and other self-aligned MOx structures," *Chemical Communications*, no. 20, pp. 2791–2808, 2009.

[9] Y.-C. Nah, I. Paramasivam, and P. Schmuki, "Doped TiO_2 and TiO_2 nanotubes: synthesis and applications," *ChemPhysChem*, vol. 11, no. 13, pp. 2698–2713, 2010.

[10] C. W. Lai and S. Sreekantan, "Preparation of hybrid WO_3-TiO_2 nanotube photoelectrodes using anodization and wet impregnation: improved water-splitting hydrogen generation performance," *International Journal of Hydrogen Energy*, vol. 38, pp. 2156–2166, 2013.

[11] C. W. Lai and S. Sreekantan, "Optimized sputtering power to incorporate WO_3 into C-TiO_2 nanotubes for highly visible photoresponse performance," *NANO*, vol. 7, no. 6, Article ID 1250051, 2012.

[12] A. Kubacka, M. Fernández-García, and G. Colón, "Advanced nanoarchitectures for solar photocatalytic applications," *Chemical Reviews*, vol. 112, no. 3, pp. 1555–1614, 2012.

[13] S. A. K. Leghari, S. Sajjad, F. Chen, and J. Zhang, "WO_3/TiO_2 composite with morphology change via hydrothermal template-free route as an efficient visible light photocatalyst," *Chemical Engineering Journal*, vol. 166, no. 3, pp. 906–915, 2011.

[14] C. W. Lai and S. Sreekantan, "Incorporation of WO_3 species into TiO_2 nanotubes via wet impregnation and their water-splitting performance," *Electrochimica Acta*, vol. 87, pp. 294–302, 2013.

[15] R. Beranek, J. M. Macak, M. Gärtner, K. Meyer, and P. Schmuki, "Enhanced visible light photocurrent generation at surface-modified TiO_2 nanotubes," *Electrochimica Acta*, vol. 54, no. 9, pp. 2640–2646, 2009.

[16] H. Song, H. Jiang, X. Liu, and G. Meng, "Efficient degradation of organic pollutant with WOx modified nano TiO_2 under visible irradiation," *Journal of Photochemistry and Photobiology A*, vol. 181, no. 2-3, pp. 421–428, 2006.

[17] W. Krengvirat, S. Sreekantan, A.-F. Mohd Noor et al., "Carbon-incorporated TiO_2 photoelectrodes prepared via rapid-anodic oxidation for efficient visible-light hydrogen generation," *International Journal of Hydrogen Energy*, vol. 37, pp. 10046–10056, 2012.

[18] M. Ni, M. K. H. Leung, D. Y. C. Leung, and K. Sumathy, "A review and recent developments in photocatalytic water-splitting using TiO_2 for hydrogen production," *Renewable and Sustainable Energy Reviews*, vol. 11, no. 3, pp. 401–425, 2007.

[19] A. Watcharenwong, W. Chanmanee, N. R. de Tacconi, C. R. Chenthamarakshan, P. Kajitvichyanukul, and K. Rajeshwar, "Anodic growth of nanoporous WO_3 films: morphology, photoelectrochemical response and photocatalytic activity for methylene blue and hexavalent chrome conversion," *Journal of Electroanalytical Chemistry*, vol. 612, no. 1, pp. 112–120, 2008.

[20] X. Zhang, K. Huo, L. Hu, and P. K. Chu, "Fabrication and photocatalytic activity of nanoporous WO_3 film," *Nanoscience and Nanotechnology Letters*, vol. 2, no. 1, pp. 51–57, 2010.

[21] L. Meda, G. Tozzola, A. Tacca et al., "Photo-electrochemical properties of nanostructured WO_3 prepared with different organic dispersing agents," *Solar Energy Materials & Solar Cells*, vol. 94, no. 5, pp. 788–796, 2010.

[22] C. W. Lai and S. Sreekantan, "Fabrication of WO_3 nanostructures by anodization for visible-light driven water splitting and photodegradation of methyl orange," *Materials Science in Semiconductor Processing*, vol. 16, pp. 303–310, 2013.

[23] W. Li, J. Li, X. Wang, S. Luo, J. Xiao, and Q. Chen, "Visible light photoelectrochemical responsiveness of self-organized nanoporous WO_3 films," *Electrochimica Acta*, vol. 56, no. 1, pp. 620–625, 2010.

[24] S. Berger, H. Tsuchiya, A. Ghicov, and P. Schmuki, "High photocurrent conversion efficiency in self-organized porous WO_3," *Applied Physics Letters*, vol. 88, no. 20, Article ID 203119, 2006.

[25] Y.-C. Nah, A. Ghicov, D. Kim, and P. Schmuki, "Enhanced electrochromic properties of self-organized nanoporous WO_3," *Electrochemistry Communications*, vol. 10, no. 11, pp. 1777–1780, 2008.

[26] T. Siciliano, A. Tepore, G. Micocci, A. Serra, D. Manno, and E. Filippo, "WO_3 gas sensors prepared by thermal oxidization of tungsten," *Sensors and Actuators B*, vol. 133, no. 1, pp. 321–326, 2008.

[27] V. Cristino, S. Caramori, R. Argazzi, L. Meda, G. L. Marra, and C. A. Bignozzi, "Efficient photoelectrochemical water splitting by anodically grown WO_3 electrodes," *Langmuir*, vol. 27, no. 11, pp. 7276–7284, 2011.

[28] C. W. Lai and S. Sreekantan, "Heat treatment effects of WO_3-loaded TiO_2 nanotubes with enhanced water splitting hydrogen generation," *Materials Science in Semiconductor Processing*, vol. 16, pp. 947–954, 2013.

[29] C. W. Lai and S. Sreekantan, "Effect of applied potential on the formation of self-organized TiO_2 nanotube arrays and its photoelectrochemical response," *Journal of Nanomaterials*, vol. 2011, Article ID 142463, 7 pages, 2011.

[30] S. Sreekantan, L. C. Wei, and Z. Lockman, "Extremely fast growth rate of TiO_2 nanotube arrays in electrochemical bath containing H_2O_2," *Journal of the Electrochemical Society*, vol. 158, no. 12, pp. C397–C402, 2011.

[31] C. W. Lai and S. Sreekantan, "Photoelectrochemical performance of smooth TiO_2 nanotube arrays: effect of anodization temperature and cleaning methods," *International Journal of Photoenergy*, vol. 2012, Article ID 356943, 11 pages, 2012.

[32] H.-J. Oh, J.-H. Lee, Y.-J. Kim, S.-J. Suh, J.-H. Lee, and C.-S. Chi, "Synthesis of effective titania nanotubes for wastewater purification," *Applied Catalysis B*, vol. 84, no. 1-2, pp. 142–147, 2008.

[33] B. Bulic, M. Pickhardt, E.-M. Mandelkow, and E. Mandelkow, "Tau protein and tau aggregation inhibitors," *Neuropharmacology*, vol. 59, no. 4-5, pp. 276–289, 2010.

[34] M. Havelcová, P. Kubát, and I. Němcová, "Photophysical properties of thiazine dyes in aqueous solution and in micelles," *Dyes and Pigments*, vol. 44, no. 1, pp. 49–54, 1999.